Preliminary Results for the First Year of Operation of a Seasonal Storage Solar Combisystem for a Single Detached House

Curtis Meister and Ian Beausoleil-Morrison

Carleton University, Ottawa (Canada)

Abstract

This work describes the operation of a solar combisystem equipped with a buried water tank for seasonal storage. The combisystem supplies space heating and domestic hot water to a single-detached house in a cold climate. The system was operated over the summer of 2017 through spring of 2018, and achieved solar fractions of 66% and 60% for space heating and domestic hot water, respectively. However, a number of issues prevented consistent operation and/or monitoring of the system, and the solar thermal array was found to underperform significantly. Thus, the results of this cycle should not be taken as the definitive performance of such a system. The data collected from the system's first year of operation will be used to develop and validate models of the seasonal storage tank and other system components.

Keywords: seasonal storage, solar thermal, solar combisystems, solar heating

1. Introduction

Our reliance on fossil fuels in the residential sector could be drastically reduced by replacing conventional space and hot water heating systems with solar combisystems. Solar combisystems provide space heating and hot water to loads through solar-thermally-charged hot water storage tanks. Solar combisystems are typically equipped with short-term heat storage, referred to herein as diurnal thermal energy storage (DTES). The DTES would consist of one or multiple hot water tanks, typically less than 1000 litres in volume. Combisystems with diurnal heat storage have usually been shown to produce solar fractions ranging from 50-60% (see: Dincer and Rosen (2011), Edwards (2014)), or in optimized cases, upwards of 70% (Ray and Zmeureanu (2018)). To meet a higher fraction of space heating and domestic hot water loads, solar combisystems will need to take advantage of excess solar heat availability in the summer. Seasonal thermal energy storage (STES) aims to do so. Rather than storing solar heat for a few days, seasonal stores should store heat for several months, such that energy is available when loads peak mid-winter.

Seasonal storage has thus become an active area of research. In the 1980s, Task 7 of the International Energy Agency's (IEA) Solar Heating and Cooling (SHC) program focused on central heating plants with STES. As a result of the program, a large number of district STES systems were installed in Europe (over 20, according to Ochs et al. (2009)). Several types of STES were built, including buried water tanks, rockpits, borehole fields, and underground water caverns (aquifers). These systems typically achieved solar fractions of 50-60% for space heating and DHW (Bauer et al (2010), Ochs et al. (2009), Schmidt et al (2004)). Nearly all of the systems reported experienced higher than expected storage losses. Ochs et al. (2009) attribute this to moisture diffusion within the storage insulation, and provides a method for calculating an estimated "effective conductivity" of moist insulation.

a) b)

Fig. 1: a) The Urbandale Centre for Home Energy Research and b) Seasonal Storage Tank Installation

doi:10.18086/eurosun2018.13.11 Available at http://proceedings.ises.org

Recent attempts at district STES have achieved a better thermal performance. The Drake Landing Solar Community (DLSC) is detailed in Mesquita et al. (2017) and Sibbitt et al. (2012). The DLSC is a 52-house community with an average heated floor area of 145 m^2. It uses 2293 m^2 of flat plate solar collectors to charge a large field of 144 boreholes used as seasonal storage. Over the past 5 years, the DLSC has achieved an average annual solar fraction of 96% for space heating (Mesquita et al. (2017)).

Seasonal storage has received less attention on the smaller single-home scale, especially in terms of experimental systems. Colcough et al. (2011) outlines a STES system that was installed on a passive house in Ireland. The system had a 10.8 m^2 evacuated tube solar array, 300 litre DTES tank and a 23 m^3 STES tank. The system achieved solar fractions of 56% and 93% for space heating and domestic hot water respectively. The researchers found that losses from the STES tank were significant, up to double the design value (Clarke (2014)). While a high solar fraction experimental combisystem was not found in the literature, several authors have presented simulated systems that have achieved high solar fractions. In the precursor to this work, Wills (2013) and Kemery (2017) simulated solar combisystems with STES for a single-detached house in Ottawa, Canada. Wills (2013) found that a flat-plate based combisystem could achieved an 89% solar fraction utilizing an 80 m^3 STES tank. Kemery (2017) simulated a STES system similar to the as-built system described in this work, and found that solar fractions over 93% were attainable. Hugo and Zmeureanu (2010) found that solar fractions of over 93% could be attained for a house in Montreal, Canada with tank sizes ranging from 27-39 m^3.

Clearly, there exists potential for STES systems to meet the majority of energy demands for single detached homes. However, this potential has not yet been demonstrated via full-scale experiment. This work aims to fill this knowledge gap. To this end, this work describes the performance of a combisystem with STES installed at the Urbandale Centre for Home Energy Research (CHEeR) in Ottawa, Canada. The system (Figure 1) features an evacuated tube solar array of gross area 43 m^2 and a buried seasonal storage tank that is approximately 36 m^3 in volume. Data on the various energy flows in the system were collected over the first proper heating season under operation. In this paper, we present the results of the heating season and identify a number of areas of underperformance.

2. Experimental Setup

2.1 Solar Combisystem with Seasonal Storage Tank

Figure 2 shows a schematic of the solar combisystem. The solar array features ten sets of 30-tube evacuated tube collectors, arranged in two parallel lines and tilted at 60°. The array can charge either the STES tank or DTES Tank A. DTES Tank A can subsequently exchange water with Tank B and C. Because a form of glycol is used in the collector loop, all solar charging is indirect, i.e. a heat exchanger and separate pump are used on the tank side of the solar charging loop. The seasonal storage tank is 36 m^3 in volume. It is buried behind the house to minimize heat losses, and has 30.5 cm of spray-on polyurethane insulation. This gives the tank a nominal U-value of 0.075 W/mK.

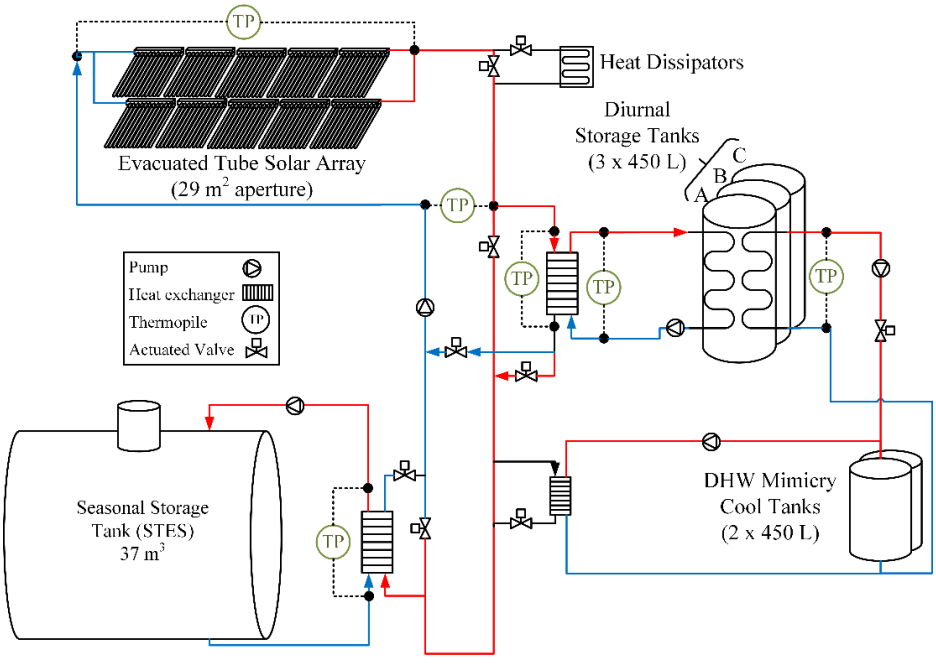

Fig. 2: Simplified schematic of CHEeR's solar thermal system with seasonal storage

Space heating is performed through a hydronic radiant floor, which can be heated by either the STES tank or through DTES Tank B or C. Thus, space heating via the DTES requires solar heat from Tank A to be transferred to Tank B or C. A small pump can move water from Tank A to either tank B or C to do so. Domestic hot water is supplied exclusively from DTES A. Because the house does not have mains water connection, mains water is mimicked. Hot water from the tank is exchanged with two cool tanks, which are cooled via the solar loop's dissipators overnight. This configuration thus limits the effectiveness of heat exchange in summer months, as the cool tanks do not always reach realistic mains water temperatures. More detail on the research house and the combisystem's instrumentation and design is provided in Meister and Beausoleil-Morrison (2017).

2.2 Control of the Solar Combisystem

Meister and Beausoleil-Morrison (2017) give the general control scheme for the combisystem used in this research. The solar pump turns on when a pyranometer senses a collector-plane irradiance of more than 150 W/m^2. The system "preheats" the solar loop until an RTD on the array senses a temperature 3°C above any active load. The system then directs flow to charge whichever load was exceeded. A priority and setpoint based system is implemented in the control scheme to help ensure both space heating and domestic hot water loads are met. The priorities for solar charging were as follows:

1. Charge DTES Tank A to 55°C to meet domestic hot water loads.
2. (If DTES Tank B/C active for space heating) Charge DTES tanks to 70°C.
3. Charge STES to 93°C.

Space heating had a similar priority system. The supply temperature for the radiant floor was 30°C. If either DTES Tanks B and C or the STES was over 30°C at its top, it was eligible for space heating. For space heating, heating via the diurnal storage is prioritized over the STES tank. If neither thermal store exceeded the desired supply temperature, the auxiliary boiler would turn on. For the heating season reported here, only DTES Tank A and B were operated. While Tank A operated throughout the season, Tank B was enabled from January 26-February 27, 2018.

2.3 Virtual DTES Tank

As many experiments take place at the CHEeR house, it was not possible to access the DTES tanks for the entire testing period. Thus, to emulate the effect of charging the diurnal storage when the real DTES was unavailable, a "virtual tank" was simulated in the control scheme. In reality, charging the virtual tank consisted of dissipating solar heat to the ambient air via the heat dissipators. The virtual tank consisted of a simple lumped-heat capacitance model of the real DTES Tank A. It would gain heat in response to the measured heat dissipation rate, and lost heat via standing losses and domestic hot water demands. When operated, the virtual DTES tank was controlled in the same fashion as the real DTES tank. The virtual tank was used in place of the real DTES from August 15 to October 16, 2017.

3. Preliminary Results

This section present preliminary results from operating the STES system through its first heating season. Results are presented starting July 27, 2017, when the data collection system was fully commissioned, through to the end of the heating season in late April. Figure 3 shows the temperature of the seasonal storage tank throughout this period. As reported in Meister and Beausoleil-Morrison (2017), a cooldown test of the seasonal storage tank was conducted from July 17 to August 7, after which charging of the STES continues. The peak temperature reached by the STES tank was approximately 80°C in early October. To begin the heating season, the DTES tanks were not yet configured to allow space heating, and thus, all space heating came from the STES tank. From the time space heating began in late October until late December, much of the tank's stored heat was already depleted. Regrettably, a key period of data (Dec 22 – Jan 4th) was lost due to a power failure. This period of data represented the coldest stretch of the year in Ottawa, with average daily temperatures falling below -25°C. It is evident from Figure 3 that the STES temperature dropped significantly over this period, falling below 30°C when data becomes available on January 5th.

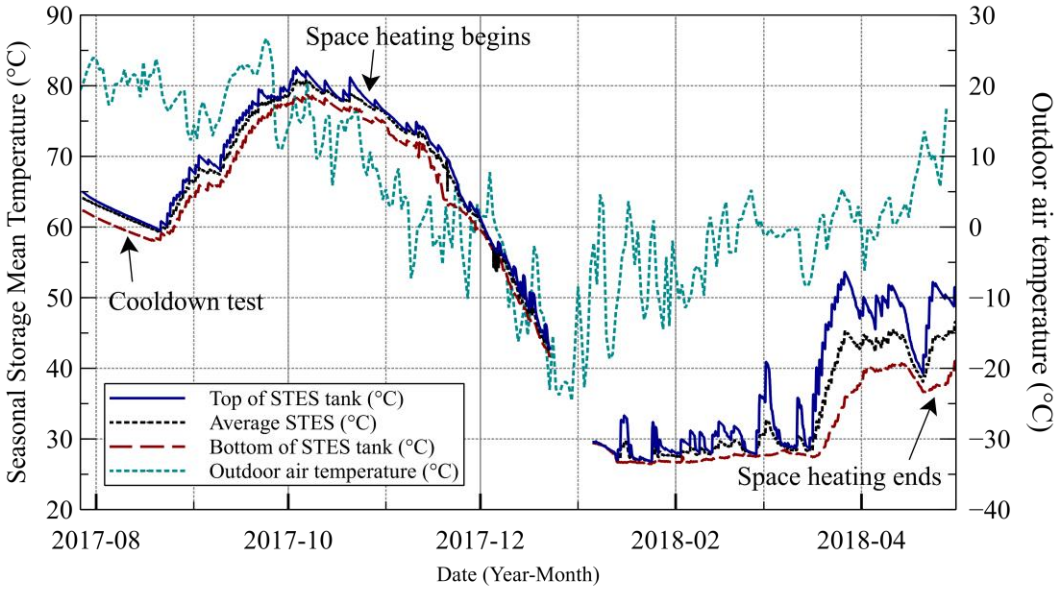

Figure 3: Seasonal storage tank and outdoor air temperatures

The diurnal storage was configured to supply space heating through DTES Tank B on January 26th. Once enabled, much of the solar heat was directed to the DTES tanks, thus the STES tank temperature remained relatively constant. DTES Tank B was enabled throughout January and February, after which the STES temperature begins to rise again. The pump speed through the STES tank was lowered from approximately 11 L/min to 5.5 L/min in February. This change can be seen to significantly increase stratification in the STES tank during charging, however, discharging appears to rapidly destroy the stratification achieved.

3.1 Solar Collection

Figure 4 presents an overview of the measured energy supplied to each storage tank throughout the period of analysis. Solar thermal generation was highest in March, when the STES was at a low temperature, and in August and September. Note that results for August only include data for 18 days of the month. Table 1 shows the number of days analyzed in each month.

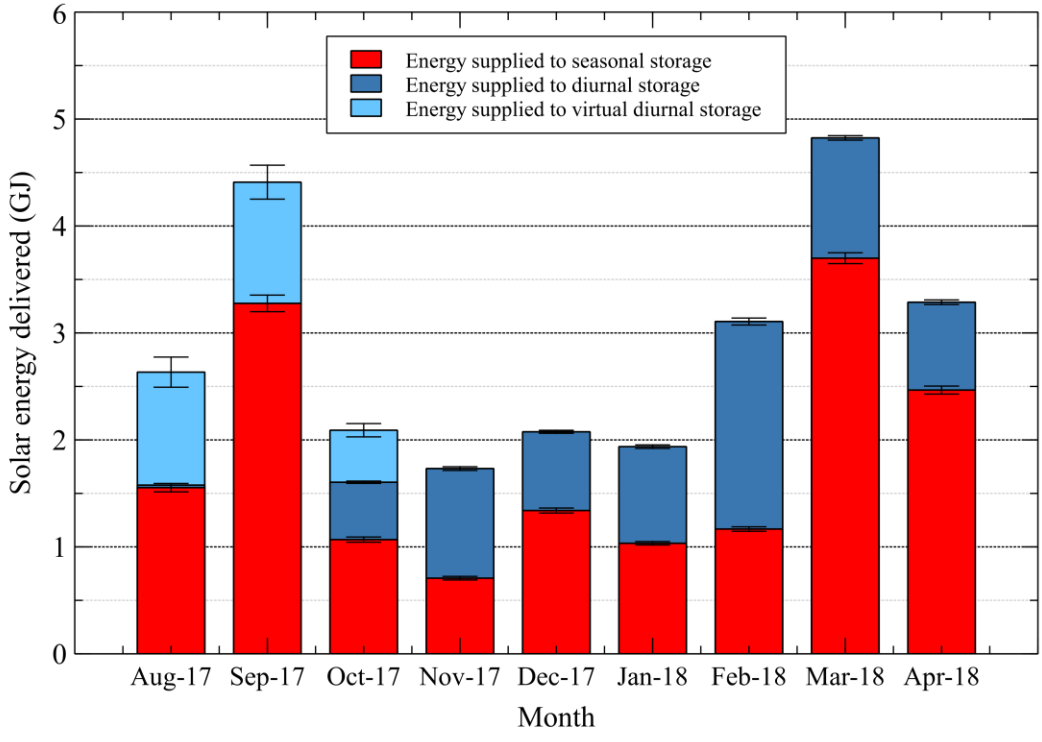

Fig. 4: Solar energy delivered to thermal storage tanks

Tab. 1: Number of days of data recorded in each month

August	September	October	November	December	January	February	March	April
18	30	30	30	22	26	27	31	29

3.2 Space Heating

Figure 5 shows the distribution of space heating energy over the analysis period. Through December, all space heating was provided by the STES tank. The space heating energy for the missing data period is not shown here, but is estimated to be approximately 2 GJ. When the STES was depleted in January, the auxiliary boiler supplied most of space heating loads until DTES Tank B was enabled on January 26. DTES Tank B remained on for nearly all February, providing 38.6% of space heating for this period. Contrasting January and February, it is evident that enabling diurnal storage for space heating improves thermal performance. The solar fractions for space heating were 29% and 52% in January and February, respectively. Notably, the measured total space heating load for the year was only 10 GJ, or approximately 12 GJ with the estimated load during the missing data period. Previous simulation work by Kemery (2017) predicted a space heating load of 20 GJ for the CHEeR house. It is likely that this difference is a function of the various internal gains in the research house, which were not considered in the simulation.

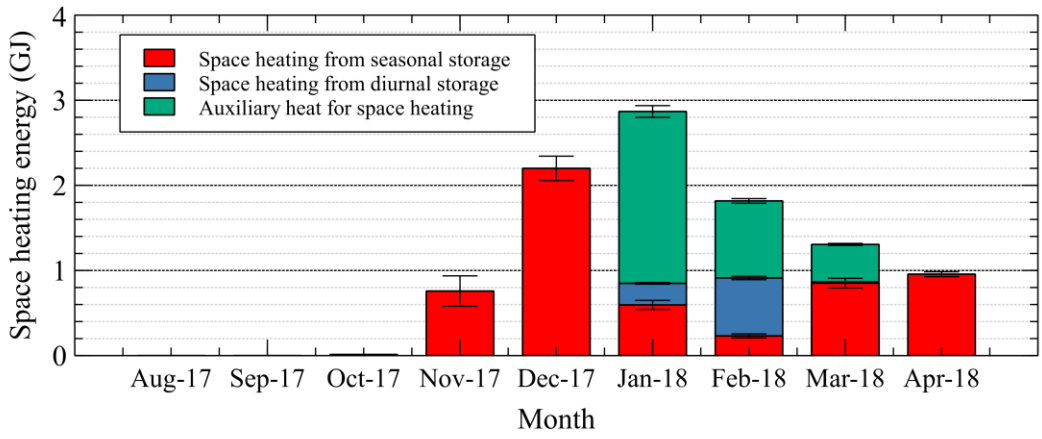

Fig. 5: Space heating energy supplied by each storage

3.3 Domestic Hot Water

Figure 6 presents the energy supplied for domestic hot water throughout the analysis period. In August and September, nearly all the DHW energy demand was met by "charging" the virtual tank. In the month of November, no domestic hot water draws were measured. However, it is believed this was due to a faulty flowmeter. Future work will attempt to identify the quantity of heat removed from DTES Tank A during this period.

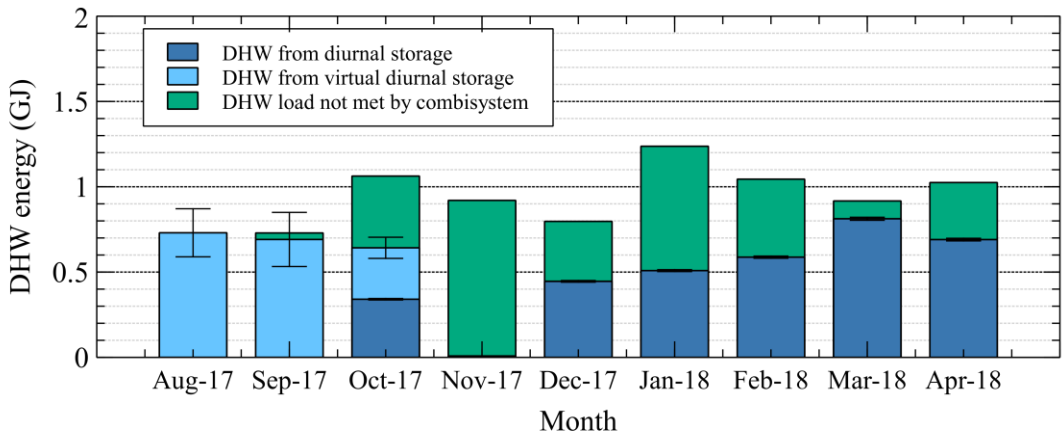

Fig. 6: Domestic hot water supplied by each storage

Further investigation into the performance of the DHW mimicry system is required to determine the relatively poor performance. It was expected that the combisystem would easily meet most DHW loads due to the large evacuated

tube array. However, certain control decisions may have hampered the system's performance. For instance, the system was constrained to only provide domestic hot water during the 5 minute interval in which a demand was present in the draw profiles. The setpoint of 55°C for diurnal storage Tank A may have also led to underperformance, as a higher setpoint may have ensured that early-morning draws were more easily met.

3.4 Summarized Results

Table 2 presents the total energy quantities measured over the analysis period. Based on the measured data, the solar fractions for space heating and domestic hot water were 66% and 60%, respectively. The overall solar fraction for the combisystem was 63%, and the total heat demand (space heating plus domestic hot water) was 18.4 GJ for the year. It must be noted that this does not include the missing data period, in which a large amount of energy was removed from the STES tank.

Tab. 2: Energy flows for the solar thermal system

Month	Solar energy addition		Space heating demands met			Domestic hot water demands met		f_{SH}	f_{DHW}	f_{tot}
	STES (GJ)	DTES (GJ)	STES (GJ)	DTES (GJ)	Boiler (GJ)	DTES (GJ)	Not met (GJ)			
August	1.55	1.08	0	0	0	0.73	0	1	1	1.00
September	3.28	1.13	0	0	0	0.69	0.04	1	0.95	0.95
October	1.07	1.02	0.01	0	0	0.64	0.42	1	0.60	0.61
November	0.71	1.02	0.76	0	0	0.01	0.91	1	0	0.46
December	1.34	0.74	2.20	0	0	0.45	0.35	1	0.56	0.88
January	1.03	0.90	0.60	0.25	2.02	0.51	0.73	0.29	0.41	0.33
February	1.17	1.94	0.23	0.68	0.91	0.59	0.46	0.49	0.56	0.51
March	3.70	1.12	0.85	0.01	0.44	0.81	0.10	0.68	0.89	0.76
April	2.47	0.82	0.96	0	0	0.69	0.33	1	0.67	0.83
Total	**16.3**	**7.11**	**5.60**	**0.95**	**3.37**	**5.11**	**3.35**	**0.66**	**0.60**	**0.63**

Table 3 shows the energy flows in and out of the STES tank, including the heat injection, removal, and losses to the ground. Heat losses are calculated from Equation 1,

$$\Delta E_{tank} = Q_{in,solar} - Q_{out,SH} - Q_{loss} \quad (1)$$

Where ΔE_{tank} represents the internal energy change in the STES tank,

$$\Delta E_{tank} = m_{tank} c_w (T_{avg,2} - T_{avg,1}) \quad (2)$$

Where m_{tank} is the mass of water in the tank and c_w is its specific heat capacity. For this simplified calculation, these are taken as constants equal to 36,300 kg and 4180 J/kgK, respectively. The variables T_{avg} represent a weighted-average of 75 thermocouples within the STES tank. Losses are especially significant in November and December, despite the tank's maximum temperatures occurring in October. However, the rate of heat loss from the STES is likely a function of the tank temperature, soil temperatures, and the temperature of the outdoor air (as the tank's hatch is above ground).

Tab. 3: Energy balance on the seasonal storage tank

Month	Solar energy in (GJ)	Space heating out (GJ)	Internal energy change (GJ)	Losses (GJ)
August	1.55	0	0.87	0.68
September	3.28	0	1.84	1.43
October	1.07	0.01	-0.52	1.57
November	0.71	0.76	-2.3	2.27
December	1.34	2.20	-2.82	1.96
January	1.03	0.60	-0.31	0.75
February	1.17	0.23	0.46	0.48
March	3.70	0.85	1.92	0.93
April	2.47	0.96	0.47	1.04
Total	**16.3 ± 0.3**	**5.60 ± 0.5**	**-0.4 ± 0.007**	**11.1 ± 0.7**

3.5 Cooldown Test

Two previous cooldown tests were reported on in Meister and Beausoleil-Morrison (2017), but it was identified that a much longer cooldown test was required to obtain a temperature drop with a smaller amount of experimental uncertainty. To further identify heat loss characteristics of the STES tank, a cooldown test was initiated on May 28, 2018. The tank began the cooldown at a temperature of 65°C, and has remained cooling since. Figure 7 shows the tank's mean temperature over 124 days of cooling. It was previously identified that the tank's nominal UA value of 4.7 W/K was unlikely to be realistic. In Figure 7, this is further evidenced; several "expected" rates of cooling are plotted for four possible mean ground temperatures. This shows that if the tank's UA value were equal to its design value, the ground temperature would have to be below 0°C and -20°C. Clearly, the UA value must be far higher than design.

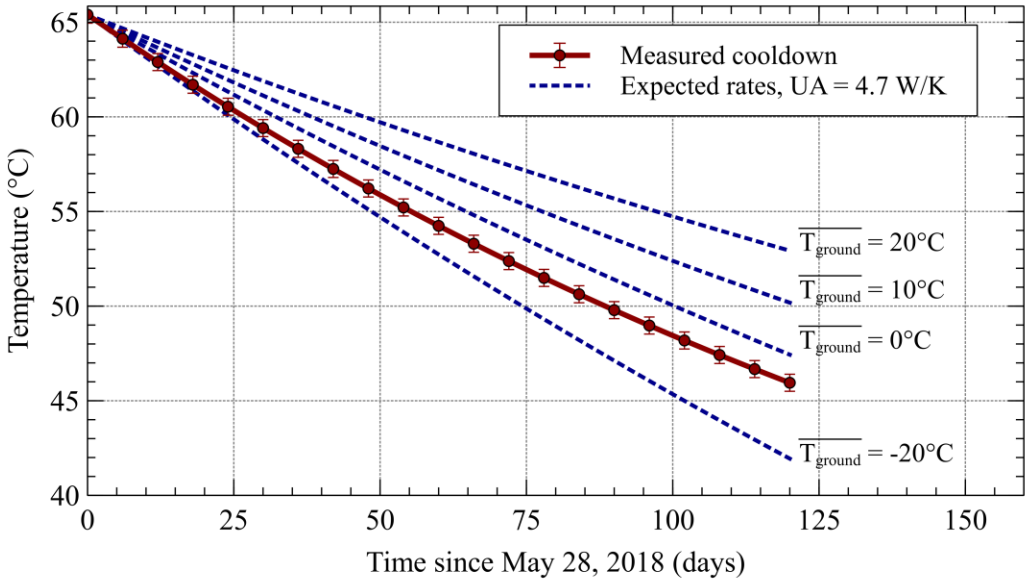

Fig. 7: Measured and predicted temperature decay of the seasonal storage tank

3.6 Solar Collector Performance

During the first year of operation of the STES system, it was noticed that the solar collectors routinely did not achieve their predicted efficiency. The collectors' ISO 9806-based efficiency equation (ISO, 2017) was obtained from the Solar Rating and Certification Corporation (SRCC) and is expressed using:

$$n_{coll} = 0.456 + 1.35090\left(\frac{\Delta T}{G}\right) - 0.00380\left(\frac{\Delta T^2}{G}\right) \quad (3)$$

Figure 8 compares the output of Equation 3 with data from the CHEeR house's solar array. Each data point represents

a point where solar collector operation was steady (less than 10% variation in efficiency) for at least 45 minutes prior to measurement. It is clear from the plot that the solar collectors did not reach their rated performance. It is estimated that the collector output was approximately 60% of the rated output. The manufacturers of the solar array have since provided replacement heat pipes for the array. They suggest that the observed underperformance could be a result of a now-outdated freeze protection process. The new heat pipes will be installed in the Fall of 2018. Based on the predictions of Kemery (2017), the authors remain optimistic that with the expected amount of solar collections, a high solar fraction can be demonstrated.

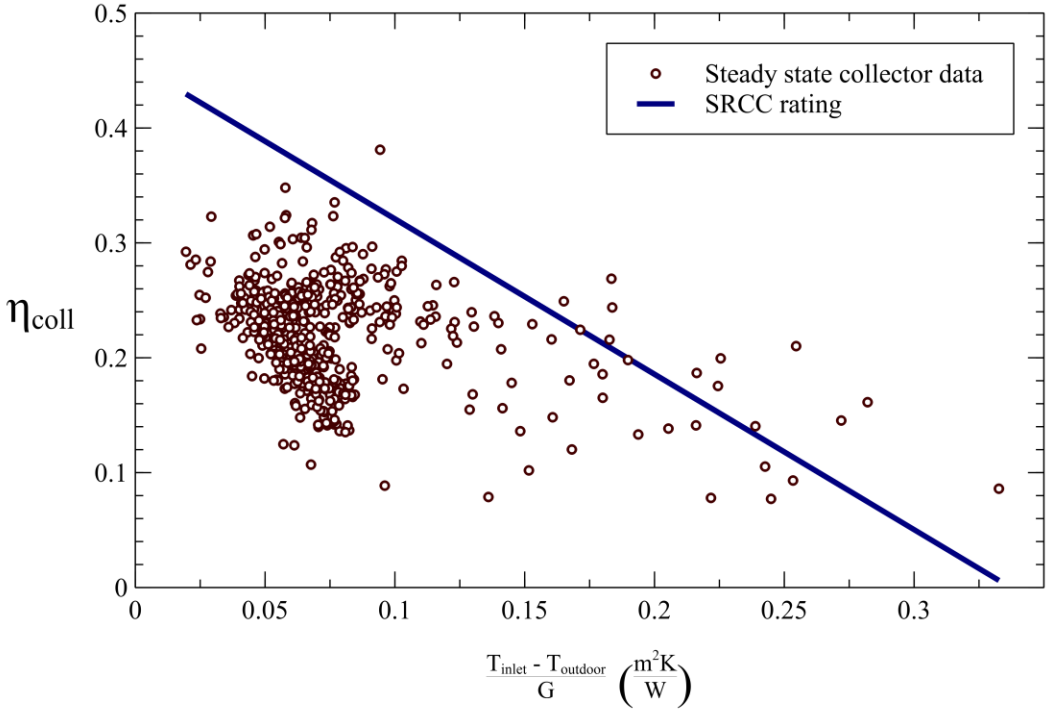

Fig. 8: Rated and measured solar collector efficiencies

3.7 Missing Data Period

Not all data was lost during the "missing data period" from December 23 to January 5th. Based on available data, the number of hours the house was receiving heat was logged, as was weather data. These are shown here to have somewhat linear effects on the space heating load and solar energy collection. Figure 9 shows the space heating load varies linearly with the number of hours in heating mode, however, the fit is not sufficient to make an accurate predictions. The solar energy collection, however, is shown to be very well predicted by the integrated radiation on the collector plane. Future work will attempt to model the full solar combisystem and CHEeR house, providing better predictions of the performance during this lost period. However, in the mean time, our best estimate of the space heating load for the missing data period is approximately 2 GJ, consistent with the internal energy lost from the STES tank over the period. Were this true, the true solar fraction for space heating would be 72% rather than 66%

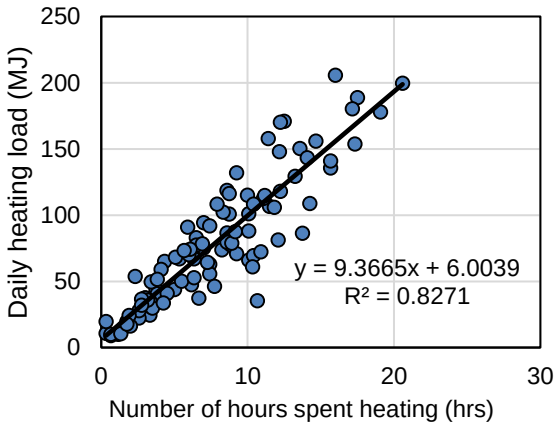

Fig. 9: Space heating load vs. heating time

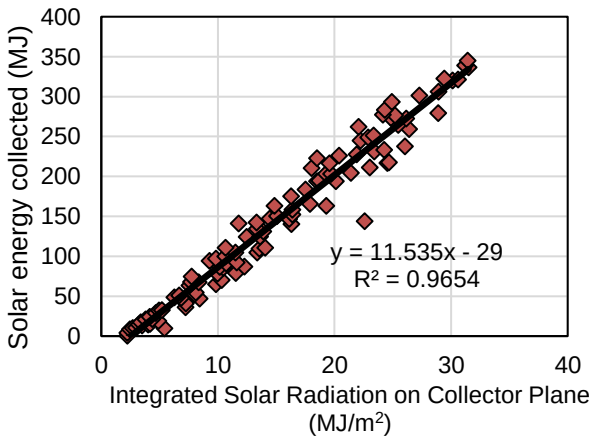

Fig. 10: Solar energy collection vs. irradiation

4. Conclusions and Outlook

The overall solar fraction was measured to be approximately 63%, far lower than the expected solar fraction of over 90%. However, several issues may have played a factor in this results. Most prominently, the solar collectors did not achieve their rated performance, meaning the solar energy input to the system was significantly less than anticipated. The work of Kemery (2016) showed that with the solar array operating at its expected performance, the STES tank would reach its maximum temperature of 93°C early into the summer, rather than struggling to reach 80°C. The effects of low solar collection were compounded by higher than expected losses from the STES tank. For the period of operation shown in this paper, losses from the STES tank were nearly double the heat extracted for space heating. Finally, the DHW system experienced some issues, including unmeasured water draws and a sub-optimal control scheme that may have restricted the energy delivery potential of the system.

As a result of this heating season, a number of methods for performance improvement have been identified. Firstly, the combisystem achieved better thermal performance when DTES Tank B was enabled to allow space heating. Were the diurnal storage allowed to provide space heating early in the heating season, the seasonal storage tank would likely not be depleted in early January, and could better serve its purpose of providing heat in mid-winter. Thus, it is recommended to enable Tank B (and possibly C) for the full heating season. Further, since the combisystem underperformed in terms of DHW loads, a higher setpoint for the diurnal storage should be investigated. Both of these recommendations fall in line with the recommendations of Dincer and Rosen (2011), who state that when storing thermal energy, one should attempt to store energy at the highest temperature possible, or at the highest exergetic state.

The results of this heating season will be used to develop a full-system model of the solar combisytem and STES tank. The model will be used to provide rapid energy predictions for the performance of the system so that a large number of control options can be explored prior to being tested on the experimental system. Based on these simulation studies, a recommended control scheme for the CHEeR STES system will be determined. With an improved control strategy and upgraded solar collectors, the CHEeR STES system may be capable of demonstrating a high solar fraction in future experiments.

5. References

Bauer, D., Marx, R., Nußbicker-Lux, J., Ochs, F., Heidemann, W. and Müller-Steinhagen, H., 2010. German central solar heating plants with seasonal heat storage. Solar Energy, 84(4), pp.612-623.

Clarke, J., Colclough, S., Griffiths, P., and McLeskey Jr., J.T., 2014. A Passive House with Seasonal Solar Energy Store: In Situ Data and Numerical Modeling, International Journal of Ambient Energy, 35(1): 37-50.

Colclough, S., Grihs, P., and Hewitt, N.,2011. A year in the life of a passive house with solar energy store. In Energy Storage Conference, (Belfast, Ireland), IC-SES.

Dincer, I. and Rosen,M., 2011 Thermal Energy Storage: Systems and Applications, second ed. John Wiley & Sons, Hoboken, NJ, USA.

Edwards, S., 2014. Sensitivity Analysis of Two Solar Combisystems Using Newly Developed Hot Water Draw Profiles. M.A.Sc Thesis, Carleton University.

Hugo, A., Zmeureanu, R. and Rivard, H., 2010. Solar combisystem with seasonal thermal storage, Journal of Building Performance Simulation, 3:4, pp.255-268.

ISO 9806. Solar energy - Solar thermal collectors - Test methods. Standard, International Organization for Standardization, 2017.

Kemery, B., 2017. Analysis and design of a solar-combisystem for high solar fraction Canadian housing with diurnal and seasonal water-based thermal stores, M.A.Sc. thesis, Carleton University.

Meister, C. and Beausoleil-Morrison, I., 2017. Experimental Characterization of a Solar Combisystem with Seasonal Storage for a Single Detached House. In Proceedings of the Solar World Congress 2017.

Mesquita, L. McClenahan, D., Thornton, J., Carriere, J. and Wong, B., 2017. Drake Landing Solar Community: 10 Years of Operation. In Proceedings of the Solar World Congress 2017.

Ochs, F., 2009. Modeling large-scale thermal energy stores. Ph.D. thesis, University of Stuttgart.

Rey, A. and Zmeureanu, R., 2018. Multi-objective optimization framework for the selection of configuration and

equipment sizing of solar thermal combisystems. Energy, 145, pp.182-194.

Schmidt, T., Mangold, D. and Müller-Steinhagen, H., 2004. Central solar heating plants with seasonal storage in Germany. Solar energy, 76(1-3), pp.165-174.

Sibbitt, B., McClenahan, D., Djebbar, R,. Thornton, J., Wong, B., Carriere, J. And Kokko, J., 2012. The performance of a high solar fraction seasonal storage district heating system - five years of operation. Energy Procedia, 30:856-865.

Wills, A., 2013. Design and co-simulation of a seasonal solar thermal system for a Canadian single-family detached house. M.A.Sc. thesis, Carleton University.